VERSITA

CELLULAR & MOLECULAR BIOLOGY LETTERS
http://www.cmbl.org.pl

Received: 13 June 2011
Final form accepted: 12 August 2011
Published online: 17 August 2011

Volume 16 (2011) pp 576-594
DOI: 10.2478/s11658-011-0024-x

Mini review

GENERALIZED STERN MODELS OF THE ELECTRIC DOUBLE LAYER CONSIDERING THE SPATIAL VARIATION OF PERMITTVITY AND FINITE SIZE OF IONS IN SATURATION REGIME

EKATERINA GONGADZE[1], URSULA VAN RIENEN[1] and ALEŠ IGLIČ[2]*
[1]Institute of General Electrical Engineering, University of Rostock, Albert-Einstein-Straße 2, 18051 Rostock, Germany, [2]Laboratory of Biophysics, Faculty of Electrical Engineering, University of Ljubljana, Tržaška 25, SI-1000 Ljubljana, Slovenia

Abstract: The interaction between a charged metal implant surface and a surrounding body fluid (electrolyte solution) leads to ion redistribution and thus to formation of an electrical double layer (EDL). The physical properties of the EDL contribute essentially to the formation of the complex implant-biosystem interface. Study of the EDL began in 1879 by Hermann von Helmholtz and still today remains a scientific challenge. The present mini review is focused on introducing the generalized Stern theory of an EDL, which takes into account the orientational ordering of water molecules. To ascertain the plausibility of the generalized Stern models described, we follow the classical model of Stern and introduce two Langevin models for spatial variation of the relative permittivity for point-like and finite sized ions. We attempt to uncover the subtle interplay between water ordering and finite sized ions and their impact on the electric potential near the charged implant surface. Two complementary effects appear to account for the spatial dependency of the relative permittivity near the charged implant surface – the dipole moment vectors of water molecules are predominantly oriented towards the surface and water molecules are depleted due to the accumulation of counterions. At the end the expressions for relative permittivity in both Langevin models were generalized by also taking into account the cavity and reaction field.

* Author for correspondence. e-mail: ales-iglic@fe.uni-lj.si , phone: +386 1 4768 825

Abbreviations used: EDL – electric double layer; LBS model – Langevin-Bikerman Stern model; LS model – Langevin Stern model; OHP – outer Helmholtz plane; PB – Poisson-Boltzmann

Key words: Spatial variation of permittivity, Generalized Stern models, Water dipoles, Charged implant surface, Osteoblasts, Cell-implant interactions, Langevin model, Langevin-Bikerman model, Booth model, Gongadze-Iglič model

INTRODUCTION

The contact between a negatively charged metal surface and an electrolyte solution results in an a rearrangement of ion distribution near the metal surface and formation of the so-called electrical double layer (EDL) [1-4]. To address the challenge of the EDL, Stern [4] combined the Helmholtz and Gouy-Chapman models, providing the first attempt to incorporate steric effects. Helmholtz [1] treated the double layer mathematically as a simple capacitor, based on a physical model in which a layer of ions with a single layer of water molecules around each ion is adsorbed at the surface. Gouy [2] and Chapman [3] considered the thermal motion of ions and pictured a diffuse double layer composed of ions of opposite charge (counterions) attracted to the surface and ions of the same charge (co-ions) repelled by it, embedded in a dielectric continuum described by the Poisson - Boltzmann (PB) differential equation. An oft-stated assumption in the models describing this phenomenon is that the permittivity of the whole system is constant. But actually, close to the charged surface the water dipoles cannot move as freely as further away from it. Besides, due to accumulation of counterions near the charged metal surface, the water molecules are partially depleted from this region. Water molecules in an electrolyte solution can also better organize their hydrogen bonding network without ions, therefore it is energetically favourable that ions which disrupt the hydrogen bonded water network are moved from the bulk towards the charged metal surface [5]. In addition, the dipole moment vectors of water molecules at the charged metal surface are predominantly oriented towards the surface, while further away from the charged surface all orientations of water dipoles are equally probable [6-9].

The present paper describes two generalized Stern models of EDL which take into account the actual spatial variation of the permittivity near the charged surface [7]. The interplay between water ordering and the finite size of ions and their impact on the decrease of permittivity near the charged surface is discussed.

STERN MODEL WITH A CONSTANT PERMITTIVITY

In this mini review, we consider a planar uniformly charged surface in contact with an electrolyte solution of ions (counterions and co-ions). The planar surface bears a charge described by the surface charge density σ_{eff}, which incorporates the negatively charged electrode, as well as the specifically bound negatively charged ions. The x-axis of the Cartesian coordinate system used points in

a direction perpendicular from the charged planar surface to the bulk solution. The electric potential in general can be calculated from Poisson's equation [10]:

$$\frac{d}{dx}\left(\varepsilon_r(x)\varepsilon_0\frac{d\phi(x)}{dx}\right)=-\rho(x), \quad (1)$$

where $\varepsilon_r(x)$ is the relative permittivity of the medium, ε_0 is the permittivity of a vacuum, $\phi(x)$ is the electric potential and $\rho(x)$ is the macroscopic (net) volume charge density in the electrolyte solution.

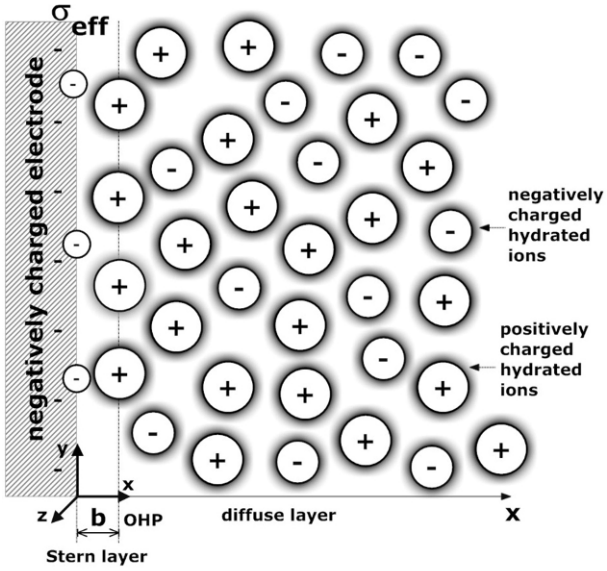

Fig. 1. Stern model consisting of a Stern layer defined by the outer Helmholtz plane (OHP) and a diffuse layer.

Generally, the Stern model [4] consists of the Stern layer, restricted by an outer Helmholtz plane (OHP) [11] (Fig. 1), where the centres of hydrated counterions are at the distance of closest approach (b). In the classical Stern model, the relative permittivity of the medium $\varepsilon_r(x)$ is considered constant over both regions: $\varepsilon_r(x)=\varepsilon_{r1}$. (2)

Within the Stern layer $(0<x<b)$ (see Fig. 1), the electric potential is described by the Poisson equation, Eq. 1. The media is considered homogeneous and the ions are assumed to have a point-like charge at their centre. As they are arranged in the OHP, the charge density within the layer is zero ($\rho(x)=0$). On the other hand, in the diffuse layer $(b<x<\infty)$, the macroscopic volume charge density has the following form:

$$\rho(x)=\sum_i v_i e_0 n_i(x) \quad (3)$$

with $n_i(x)$ being the concentration of the ions, $i = +/-$ the counterions and co-ions respectively, e_0 the elementary charge and ν_i the ion valence. Hereafter, we assume that the ions are monovalent and their valence ν_i is equal to $\nu_+ = 1$ and $\nu_- = -1$ for positive and negative ions respectively. The number density (i.e. the number of molecules per unit volume) of the charged ions of the electrolyte solution obeys the Boltzmann distribution law:

$$n_i(x) = n_0 \exp(-\nu_i e_0 \phi(x)\beta), \qquad i = +,-, \tag{4}$$

where $\beta = 1/kT$ and k is the Boltzmann constant, T the absolute temperature and n_0 the number density of ions in the bulk far away from the charged surface. Within the whole paper, we use a Cartesian coordinate system. By combining Eqs. 1-4, we obtain the so-called Poisson-Boltzmann equation (PB) for the region $b < x < \infty$. The equations describing the Stern model are obtained then as

$$\frac{d^2\phi}{dx^2} = \begin{cases} 0 & 0 \le x < b \\ \dfrac{2n_0 e_0}{\varepsilon_{r1}\varepsilon_0} \sinh(e_0\phi(x)\beta) & b \le x < \infty \end{cases} \tag{5}$$

At room temperature the relative permittivity ε_{r1} (Eq. 2) is equal to 78.5. The boundary condition at x = 0 is consistent with the condition of electroneutrality of the whole system:

$$\left.\frac{d\phi}{dx}\right|_{x=0} = -\frac{\sigma_{eff}}{\varepsilon_{r1}\varepsilon_0}. \tag{6}$$

The validity of Gauss's law at $x = b$ is fulfilled by the following equations:

$$\left.\frac{d\phi}{dx}\right|_{b_-} = \left.\frac{d\phi}{dx}\right|_{b_+}, \tag{7}$$

where also $\phi|_{b_-} = \phi|_{b_+}$. Due to screening of the negatively charged metal surface by the accumulated cations, far away from the charged metal surface the magnitude of the electric field strength $E = |d\phi/dx|$ tends to zero and consequently the electric potential there is constant. For simplicity we choose the value of electric potential to be zero at $x \to \infty$:

$$\phi|_{x\to\infty} = 0. \tag{8}$$

The classical Stern model described above treats the electrolyte solution as a continuous medium with a constant relative permittivity, i.e. it totally neglects the finite size of the ions, as well as the orientational ordering of water molecules close to the charged metal surface [7]. Ignoring the influence of the orientational ordering of water molecules is certainly a very rough

approximation, which is reflected in considerable discrepancies between the measured and predicted values of the surface electric potential, as well as in the corresponding values of the concentration of ions near the charged surface [7, 8, 11, 12]. Namely, the free rotation of polar water molecules is due to the strong electric field being substantially hindered at the charged metal surface. In addition, the strong accumulation of counterions near the charged surface may drastically reduce the concentration of water molecules at the charged metal surface [13-16]. Both phenomena, which are not taken into account in the classical Stern model, strongly influence the relative permittivity and the electric potential near the charged metal surface [7, 11, 16, 17]. Therefore, in the following sections we describe the influence of the finite size of ions and the orientational ordering near the charged metal surface on the spatial variation of permittivity. At the end the classical Stern model is generalized to take into account the spatial variation of permittivity near the charged metal surface.

SPATIAL VARIATION OF PERMITTIVITY FOR POINT-LIKE IONS - LANGEVIN MODEL

In the previous section describing the classical Stern model, the relative permittivity was taken into account a priori rather than deriving it from the average microscopic charge density, as is actually done in the present Langevin-Boltzmann model of permittivity of an electrolyte solution in contact with a charged surface for point-like ions [7]. In the Langevin- Boltzmann model the electrolyte solution consists of water molecules, monovalent cations and anions. As already mentioned above, it was indicated [7] that the permittivity profile close to the charged surface is mainly determined by two mechanisms: the depletion of the water dipoles at the charged surface due to accumulation of counterions, and the decrease in orientational ordering of the water dipoles as a function of the increasing distance from the charged metal surface.

In order to derive the spatial variation of the relative permittivity, the polarization $P(x)$ is written as

$$P(x) = n_{0w} \left\langle \mathbf{p}(x,\omega) \right\rangle_B , \qquad (9)$$

where n_{0w} is the number density of water dipoles, $\mathbf{p}(x,\omega)$ is the water (Langevin) dipole moment vector at coordinate x, angle ω describes the orientation of the dipole moment vector with respect to the x-axis and $\left\langle \mathbf{p}(x,\omega) \right\rangle_B$ is the average of $\mathbf{p}(x,\omega)$ over the angle distribution in thermal equilibrium at given x. In our case of a negatively charged planar surface ($\sigma_{eff} < 0$), the electric field strength vector $\mathbf{E}$ and the projection of the polarization vector $\mathbf{P}$ point in the direction opposite to the direction of the x-axis. Hence $P(x)$ is considered negative.

The probability of finding a water dipole vector in an element of solid angle $d\Omega = 2\pi \sin\omega \, d\omega$ is proportional to the Boltzmann factor $\exp(-W_d\beta)$, where

$$W_d = -\mathbf{p}\cdot\mathbf{E} = \mathbf{p}\cdot\nabla\phi = p_0 E\cos(\omega) \quad (10)$$

is the energy of the water (Langevin) dipole $\mathbf{p}$ in the electric field $\mathbf{E} = -\nabla\phi$, $E = |\phi'|$ is the magnitude of the electric field strength, ϕ' is the first derivative of ϕ with respect to x and p_0 is the magnitude of the water dipole moment. Hence:

$$\langle \mathbf{p}(x,\omega)\rangle_B = \frac{\int_0^{\pi} p_0\cos\omega \, \exp(-p_0 E\beta\cos\omega) 2\pi\sin\omega \, d\omega}{\int_0^{\pi} \exp(-p_0 E\beta\cos\omega) 2\pi\sin\omega \, d\omega} = -p_0 \mathrm{L}\left(p_0 E\beta\right). \quad (11)$$

In our case $\sigma_{eff} < 0$ and $\phi' > 0$: $E = |\phi'| = \phi'$. The function $\mathrm{L}(u) = \left(\coth(u) - 1/u\right)$ is the Langevin function, which describes the average magnitude of the Langevin dipole moments for a given $\mathrm{E(x)}$. In the derivation of Eq. 11, we assumed that for a given ω the dipole moment vector $\mathbf{p}$ is oriented uniformly around the x-axis. By substituting Eq. 11 into Eq. 9, we can express the polarization as:

$$P(x) = n_{0w}\langle \mathbf{p}(x,\omega)\rangle_B = -n_{0w} p_0 \mathrm{L}\left(p_0 E\beta\right). \quad (12)$$

The relative permittivity of the electrolyte solution ($\varepsilon_r(x)$) can be derived as [10]:

$$\varepsilon_r = 1 + \frac{|P|}{\varepsilon_0 E}. \quad (13)$$

By taking into consideration Eq. 13, the relative permittivity takes the following form [7]: $\varepsilon_r(x) = 1 + \frac{|P|}{\varepsilon_0 E} = 1 + n_{0w}\frac{p_0}{\varepsilon_0}\frac{\mathrm{L}(p_0 E\beta)}{E}$. (14)

For $p_0 E\beta = 1$ we can expand the Langevin function in Eq. 14 into a Taylor series up to the cubic term: $\mathrm{L}(u) \approx x/3 - x^3/45$ to get [7]:

$$\varepsilon_r(x) \approx 1 + n_{0w}\beta p_0^2/3\varepsilon_0 - n_{0w}\beta p_0^2 (p_0 E\beta)^2/45\varepsilon_0. \quad (15)$$

Obviously, from Eq. 15 it may be deduced that the relative permittivity $\varepsilon_r(x)$ decreases with increasing magnitude of the electric field strength (E). Since the electric field strength $\mathbf{E}$ decreases with increasing distance from the charged metal surface, this means that $\varepsilon_r(x)$ increases with increasing distance from the charged surface. In accordance with the results of other authors (see for example

[9, 11]), it can be concluded that due to the distinct preferential orientation of water dipoles in the close vicinity of the charged surface, the relative permittivity $\varepsilon_r(x)$ is reduced relative to its bulk value [7].

SPATIAL VARIATION OF PERMITTIVITY FOR FINITE-SIZED IONS – THE LANGEVIN-BIKERMAN MODEL

To develop an integrating framework to clarify the factors influencing the relative permittivity, in this section we derive the permittivity with a spatial variation taking into account the orientational ordering of water and the finite size of molecules (Langevin-Bikerman model [7, 17]. The finite size of molecules is considered by assuming that ions and dipoles are distributed in a lattice, where each lattice belongs to only one of three molecular species (cations, co-ions, water molecules) [6, 7, 13, 14-16].

Since in bulk solution the number densities of water molecules (n_{0w}), counterions (n_0) and co-ions (n_0) are constant, their number densities can be expressed in a simple way by calculating the corresponding probabilities that a single lattice site is occupied by one of the three particle types in the electrolyte solution (counterions, co-ions and water molecules):

$$n_+(x\to\infty) = n_-(x\to\infty) = n_s \frac{n_0}{n_0 + n_0 + n_{0w}}, \tag{16}$$

$$n_w(x\to\infty) = n_s \frac{n_{0w}}{n_0 + n_0 + n_{0w}}, \tag{17}$$

where n_s is the number density of lattice sites defined as $n_s = 2n_0 + n_{0w}$. The number densities of ions and water molecules are influenced by the charged surface so the probabilities that the single lattice site is occupied by one of the three kinds of particles should be corrected by the corresponding Boltzmann factors:

$$n_+(x) = n_s \frac{n_0 e^{-e_0\phi\beta}}{n_0 e^{e_0\phi\beta} + n_0 e^{-e_0\phi\beta} + n_{0w}\left\langle e^{-p_0 E\beta\cos\omega}\right\rangle_\omega}, \tag{18}$$

$$n_-(x) = n_s \frac{n_0 e^{e_0\phi\beta}}{n_0 e^{e_0\phi\beta} + n_0 e^{-e_0\phi\beta} + n_{0w}\left\langle e^{-p_0 E\beta\cos\omega}\right\rangle_\omega}, \tag{19}$$

$$n_w(x) = n_s \frac{n_{0w}\left\langle e^{-p_0 E\beta\cos\omega}\right\rangle_\omega}{n_0 e^{e_0\phi\beta} + n_0 e^{-e_0\phi\beta} + n_{0w}\left\langle e^{-p_0 E\beta\cos\omega}\right\rangle_\omega}, \tag{20}$$

where

$$\left\langle e^{-p_0 E\beta\cos\omega}\right\rangle_\omega = \frac{2\pi\int_{\pi}^{0} d(\cos\omega)e^{-p_0 E\beta\cos\omega}}{4\pi} = \frac{1}{p_0 E\beta}\sinh(p_0 E\beta). \quad (21)$$

Here, $\left\langle e^{-p_0 E\beta\cos\omega}\right\rangle_\omega$ is the dipole Boltzmann factor after rotational averaging over all possible angles ω . Using the definition

$$\mathrm{H}\left(\phi,E\right)= 2n_0\cosh(e_0\phi\beta)+n_{0w}\frac{\sinh(p_0E\beta)}{(p_0E\beta)}, \quad (22)$$

Eqs. 18-20 can be written in the form [7, 17]:

$$n_+(x) = n_0\, e^{-e_0\phi\beta}\frac{n_s}{\mathrm{H}}, \quad (23)$$

$$n_-(x) = n_0\, e^{e_0\phi\beta}\frac{n_s}{\mathrm{H}}, \quad (24)$$

$$n_w(x) = \frac{n_{0w}\,n_s}{\mathrm{H}}\frac{1}{p_0E\beta}\sinh(p_0E\beta). \quad (25)$$

In the case of finite sized ions, the polarization $P(x)$ (Eq. 9) is derived as:

$$P(x) = n_w(x)\left\langle\mathbf{p}(x,\omega)\right\rangle_B = -\frac{n_{0w}\,n_s}{\mathrm{H}}\frac{1}{E\beta}\sinh(p_0E\beta)\mathrm{L}\left(p_0E\beta\right). \quad (26)$$

Based on Eq. 13, we can express the relative permittivity of the electrolyte solution ($\varepsilon_r(x)$) in contact with the charged surface as [7, 17]:

$$\varepsilon_r(x)= 1+\frac{|P|}{\varepsilon_0 E}= 1+n_s n_{0w}\frac{p_0}{\varepsilon_0}\frac{\mathrm{F}\,(p_0E\beta)}{\mathrm{H}\left(\phi,E\right)E}, \quad (27)$$

where

$$\mathrm{F}\,(u) = \mathrm{L}(u)\sinh u/u. \quad (28)$$

In the approximation of small electrostatic energy and small energy of dipoles in the electric field compared to the thermal energy, i.e. small $e_0\phi\beta$ and small $p_0E\beta$, Eq. 27 can be expanded in a Taylor series to get (for $n_s \cong n_{0w}$) [7]:

$$\varepsilon_r(x)\approx 1+n_{0w}\beta p_0^2/3\varepsilon_0 - n_{0w}\beta p_0^2(p_0E\beta)^2/45\varepsilon_0 - n_{0w}\beta p_0^2(e_0\phi\beta)^2/3\varepsilon_0. \quad (29)$$

To draw consistent inferences, we should have a closer look at Eq. 15 and Eq. 29 describing the relative permittivity for point-like and finite-sized ions,

respectively. The first three terms in the expressions for $\varepsilon_r(x)$ are equal in both models, i.e. in the Langevin model considering only orientational ordering of water and neglecting the finite size of molecules, and in the generalized Langevin model which also takes into account the finite size of molecules in the electrolyte solution. So these terms represent the effect of the orientation of water molecules in the electric field near the charged surface. The fourth term in Eq. 29 describes the decrease of $\varepsilon_r(x)$ near the charged surface due to the depletion of water dipoles because of the accumulated counterions. Therefore, based on Eqs. 15 and 29 and numerical calculations presented in [7], it can be concluded that the relative permittivity of the electrolyte solution $\varepsilon_r(x)$ near the charged metal surface is reduced relative to its bulk value due to the preferential orientation of water molecules and the depletion of water molecules in the close vicinity of the charged surface. In the following we shall present a generalization of the Stern model Fig. 2 which also includes the spatial variation of the relative permittivity $\varepsilon_r(x)$.

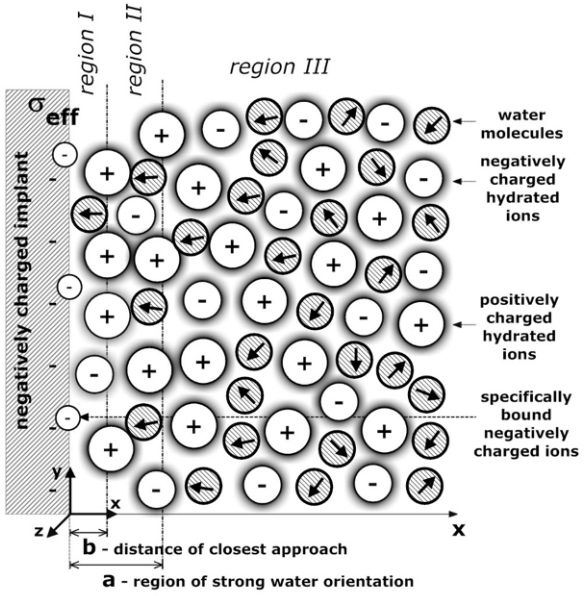

Fig. 2. Charge distribution in the generalized Stern model, where the interval $0 < x < a$ is the region of strong water orientation and b is the distance of closest approach.

GENERALIZED STERN MODELS WITH SPATIAL VARIATION OF PERMITTIVITY FOR POINT-LIKE AND FINITE SIZED IONS

Similarly as in the Stern model, so also in the generalized Stern models presented in this section the hard core interactions between the cations and the

negatively charged surface with surface charge density σ_{eff} is taken into account by means of the distance of closest approach $b \le a$, where a (or the region of preferentially oriented water molecules) is defined as in Fig. 2. The generalized Stern model model can be described consistently by dividing the half-space into three regions: region I ($0 < x < b$), region II ($b < x < a$) and region III ($a < x < \infty$). In the region $0 < x < b$, unlike in the Stern model, we still have a very small contribution to the macroscopic charge density from the few anions, despite the strong repulsion. The relative permittivity here is ε_{r2} and is smaller than the bulk value $\varepsilon_{r1} = 78.5$ (at room temperature) due to the strongly oriented water molecules and the depletion of water molecules, as described in previous sections and in [7]. The macroscopic charge density in region II is due to the cations and the few anions. The influence of the water dipoles in this region is described by $\varepsilon_{r2} < \varepsilon_{r1}$. The third region involves the cations, anions and bulk water and is described by $\varepsilon_{r1} = 78.5$, similarly to the Stern model (Fig. 2). Based on the results of statistical mechanical calculations of water ordering in an electrolyte solution near a charged surface in the previous two sections and in [7], the permittivity in generalized Stern models may therefore be approximately described as a step function of the distance from the charged surface (Fig. 3):

$$\varepsilon_r(x) = \begin{cases} \varepsilon_{r2} & x < a \\ \varepsilon_{r1} & x \ge a \end{cases} . \qquad (30)$$

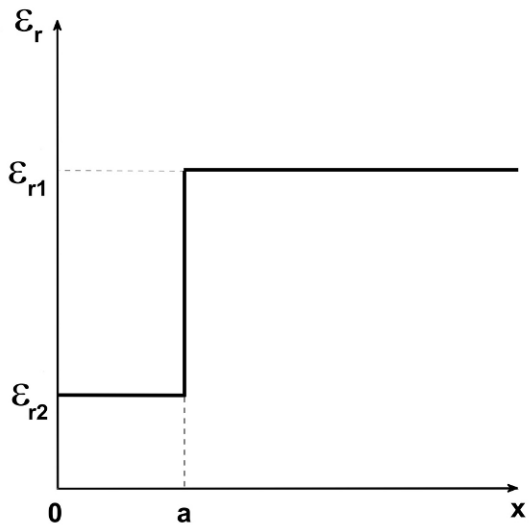

Fig. 3. Model of the relative permittivity $\varepsilon_r(x)$ in generalized Stern models as a step function of the distance from the charged surface, where a denotes the region of preferentially oriented water molecules.

Langevin Stern (LS) model for point-like ions

Similarly as in the classical Stern model for point-like ions, we combine Eqs. 1, 3 and 4 to determine the governing equations of the Langevin Stern model for point-like ions:

$$\frac{d^2\phi}{dx^2} = \begin{cases} \dfrac{e_0 n_0}{\varepsilon_{r2}\varepsilon_0}\exp\left(\beta e_0\phi(x)\right) & 0 \le x < b \\ -\dfrac{2e_0 n_0}{\varepsilon_{r2}\varepsilon_0}\sinh(\beta e_0\phi(x)) & b \le x < a \\ -\dfrac{2e_0 n_0}{\varepsilon_{r1}\varepsilon_0}\sinh(\beta e_0\phi(x)) & a \le x < \infty \end{cases} \tag{31}$$

Note that in the Poisson equation (Eq. 1) the macroscopic volume charge density $\rho(x) = e_0(n_+(x) - n_-(x))$ in the three described regions (Fig. 2) was calculated by using the Boltzmann distribution function for point-like ions (Eq. 4). Accordingly, the value of ε_{r2} should also be determined from the corresponding equation for point-like ions, i.e. from Eq. 14 as follows:

$$\varepsilon_{r2} = \varepsilon_r(x=0) = 1 + n_{0w}\frac{p_0}{\varepsilon_0}\frac{\mathrm{L}(p_0 E(x=0)\beta)}{E(x=0)} \quad . \tag{32}$$

Langevin-Bikerman Stern (LBS) model for finite-sized ions

On the other hand, for finite-sized ions the macroscopic volume charge density $\rho(x) = e_0(n_+(x) - n_-(x))$ in the Poisson equation (Eq. 1) should be calculated from the ion distribution functions for finite sized ions, i.e. from Eqs. 23 and 24. The corresponding Poisson equation (Eq. 1) then reads:

$$\frac{d^2\phi}{dx^2} = \begin{cases} \dfrac{e_0 n_0 n_s}{\varepsilon_{r2}\varepsilon_0}\dfrac{\exp\left(\beta e_0\phi(x)\right)}{\mathrm{H}\left(\phi(x), E(x)\right)} & 0 \le x < b \\ -\dfrac{2e_0 n_0 n_s}{\varepsilon_{r2}\varepsilon_0}\dfrac{\sinh(\beta e_0\phi(x))}{\mathrm{H}\left(\phi(x), E(x)\right)} & b \le x < a \\ -\dfrac{2e_0 n_0 n_s}{\varepsilon_{r1}\varepsilon_0}\dfrac{\sinh(\beta e_0\phi(x))}{\mathrm{H}\left(\phi(x), E(x)\right)} & a \le x < \infty \end{cases} \tag{33}$$

Here the value of permittivity ε_{r2} is determined from the corresponding equation for finite-sized ions, i.e. from Eq. 27 as follows:

$$\varepsilon_{r2} = \varepsilon_r(x=0) = 1 + n_s n_{0w}\frac{p_0}{\varepsilon_0}\frac{\mathrm{F}\ (p_0\beta E(x=0))}{\mathrm{H}\left(\phi(x=0), E(x=0)\right)\ E(x=0)}. \tag{34}$$

Boundary conditions

The boundary conditions in the generalized Stern models are consistent with the ones used in the Stern model. The only difference is that at $x = 0$ the relative permittivity corresponds to ε_{r2} and we can write Eq. 6 as:

$$\left.\frac{d\phi}{dx}\right|_{x=0} = -\frac{\sigma_{eff}}{\varepsilon_{r2}\varepsilon_0}. \tag{35}$$

The validity of Gauss's law should be fulfilled not only at $x = b$ (see Eq. 7), but also at $x = a$:

$$\varepsilon_{r2}\left.\frac{d\phi}{dx}\right|_{a_-} = \varepsilon_{r1}\left.\frac{d\phi}{dx}\right|_{a_+}, \tag{36}$$

where also $\phi|_{a_-} = \phi|_{a_+}$. The assumption that the electric field strength tends to zero (Eq. 7) far away from the charged metal surface is valid here as well.

The generalized Stern equations for point-like ions (Eqs. 31, 32) and finite sized ions (Eqs. 33, 34) were solved numerically for planar geometry using the finite element method (FEM) within the program package Comsol Multiphysics 3.5a Software (COMSOL AB, Stockholm). The value of ε_{r2} for a given σ_{eff} was determined in an iterative procedure, where the initial value of ε_{r2} was equal to the permittivity of the bulk solution. The corresponding boundary conditions as described above were taken into account.

Fig. 4 shows the electric potential as a function of the distance from the planar charged surface (x) calculated within the classical Stern model and both generalized Stern models, i.e. within the Langevin Stern (LS) model for point-like ions and the Langevin-Bikerman Stern (LBS) model for finite-sized ions. For both generalized Stern models the values of the relative permittivity ε_{r2} in the region $0 \le x < a$ were determined as described above, while in the classical Stern model the relative permittivity is constant in the whole solution. We should also note that within the generalized Stern models a smaller permittivity ε_{r2} yields a more negative surface potential than in the classical Stern model. Furthermore, the potential drop near the charged surface is the largest in the case of the LBS model for finite sized ions, while for point-like ions the potential drop is smaller. This can be explained by the larger value of ε_{r2} for point-like ions (see also [7]). The difference between the values of the predicted surface potential in the LS and LBS models is more pronounced for more negative surface charge densities (σ_{eff}).

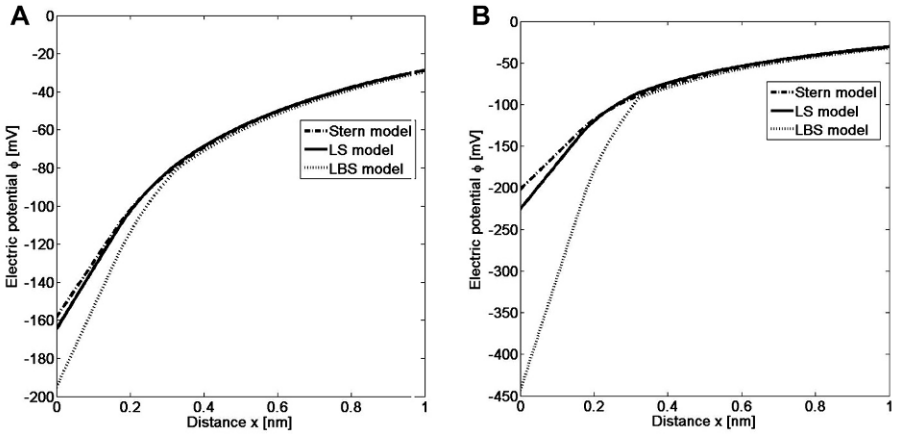

Fig. 4. Electric potential distribution in a classical Stern model (dash-dotted line) and both generalized Stern models, i.e. the Langevin Stern (LS) model for point-like ions (full line) and Langevin-Bikerman Stern (LBS) model for finite-sized ions (dashed line). In Fig. 4A the parameters used are surface charge denisty $\sigma_{eff} = -0.2\ \mathrm{As/m^2}$, ε_{r2} = 72 (for LS) and ε_{r2} = 54 (for LBS) and for Fig. 4B - surface charge denisty $\sigma_{eff} = -0.3\ \mathrm{As/m^2}$, ε_{r2} = 62 (for LS) and ε_{r2} = 25 (for LBS). The common parameters in both figures are as following: bulk concentration of salt n_0/N_A = 0.15 mol/l, $a = 0.32$ nm, $b = 0.16$ nm, $p_0 = 4.79$ D and bulk concentration of water n_{0w}/N_A = 55 mol/l.

As expected, the electric potential changes linearly in the region $0 \le x < b$, but then close to the region around $x = b$, the slope (i.e. the electric field strength) changes (see Fig. 4). The main reason for such behaviour is that the electric field strength close to the charged surface in the region $0 \le x < b$ (where the free co-ions are almost depleted) is practically completely determined by the boundary condition at the charged metal surface (at $x = 0$). Therefore, in this region the magnitude of the electric field strength is $E = d\phi / dx\big|_{x=0} = -\sigma_{eff} / \varepsilon_{r2}\varepsilon_0$.

DISCUSSION AND CONCLUSIONS

In conclusion, we have presented the generalized Langevin Stern (LS) model and the generalized Langevin-Bikerman Stern (LBS) model, in which the relative permittivity is spatially dependent and derived from the Langevin model for point-like ions and the Langevin-Bikerman model for finite sized ions. The Langevin model for point-like ions describes the influence of water dipole ordering near a charged surface on the spatial variation of the relative permittivity $\varepsilon_r(x)$. The analytical expression derived (Eq. 14) is then compared with the corresponding expression within the Langevin-Bikerman model for finite-sized ions (Eq. 27). In order to elucidate the influence of the finite size of

the ions on the relative permittivity $\varepsilon_r(x)$, $\varepsilon_r(x)$ is expanded in both models into Taylor series for small $p_0 E\beta$ and small $e_0\phi\beta$, i.e. for small magnitudes of the surface charge density σ_{eff}. The important role of water molecule depletion (4th term in Eq. 29) in the decrease of the relative permittivity near the charged surface is revealed and is even more pronounced at higher values of σ_{eff} (see [7]). The influence of water ordering (3rd term in Eqs. 15 and 29) is less important. Accordingly, a stronger decrease of the relative permittivity $\varepsilon_r(x)$ is observed near the charged surface with increasing surface charge density $\left|\sigma_{eff}\right|$ for finite-sized ions than for point-like ions [7].

As described, the contact between a negatively charged metal surface and an electrolyte solution results in a rearrangement of the ion distribution and water orientational ordering near the metal surface. A variety of EDL models have been published up to date, most of which are based on the supposition that the permittivity is constant in the whole system. However, the Langevin and Langevin-Bikerman models presented in this mini review show that the dipole moment vectors of water molecules at the charged metal surface are on average oriented towards the surface. Additionally, due to the accumulation of counterions near the charged metal surface, we predicted that the permittivity is significantly reduced there [7]. Importantly, the models of $\varepsilon_r(x)$ presented enable us to understand the basic mechanisms explaining the behaviour of the permittivity. To conclude, an important feature that results in better agreement between EDL theory and the corresponding experiments is the inclusion of spatially dependent permittivity in the theoretical EDL models [7-9, 17].

The magnitude of the effective dipole moment of the water molecule (p_0) should be known before a satisfactory statistical-mechanical study of water and aqueous solutions is possible. The dipole moment of a water molecule in liquid water differs from that of the isolated molecule because each molecule is further polarized by the electric field of the surrounding molecules [18]. Thus in the above described treatment of water ordering, in the saturation limit at high electric field within the Langevin and Langevin-Bikerman models the effective dipole moment of water $p_0 = 4.79\,\mathrm{D}$ is larger than the dipole moment of an isolated water molecule $p_0 = 1.85\,\mathrm{D}$. However, it is also larger than the dipole moment of a water molecule in clusters ($p_0 = 2.7\,\mathrm{D}$) and the dipole moment of an average water molecule in the bulk ($p_0 = 2.4 - 2.6\,\mathrm{D}$) [19] since the cavity and reaction fields, as well as structural correlations between water dipoles [20, 21], were not explicitly taken into account in the Langevin and Langevin-Bikerman models. In the past the treatment of the cavity and reaction fields and the structural correlations between water dipoles in the Onsager [22], Kirkwood [23] and Fröhlich [20] models were limited to the case of small electric field

strengths, i.e. they were valid far away from the saturation regime considered in the Langevin-Bikerman model and also in the Langevin model. Generalization of the Kirkwood-Onsager-Fröhlich theory in the saturation regime was performed by Booth [24] to find :

$$\varepsilon_r(x) = n^2 + \frac{7 n_{0w} p_0 (n^2+2)}{3\sqrt{73}\varepsilon_0} \frac{\mathrm{L}\left(\sqrt{73}(n^2+2) p_0 E\beta / 6\right)}{E}. \quad (37)$$

The above Booth expression for the relative (effective) permittivity for point-like ions takes into account the cavity and reaction fields and the structural correlations between water dipoles, and can be used instead of Eq. 14 in the LS model. In the limit of zero electric field the above equation transforms into:

$$\varepsilon_r \approx n^2 + \frac{7(2+n^2)^2 n_{0w} p_0^2 \beta}{54\varepsilon_0}. \quad (38)$$

It follows from Eq. 38 that the dipole moment of water $p_0 = 2.03$ D corresponds to the bulk permittivity $\varepsilon_r = 78.5$. Booth's expression for the relative permittvity (Eq. 37), however does not consider the excluded volume principle in electrolyte solution near a charged surface as is taken into account in the Langevin-Bikerman model (Eq. 27). Therefore the Langevin-Bikerman expression for relative permittivity was recently generalized by Gongadze and Iglič by taking into account the cavity and reaction fields (but not also structural correlations between water dipoles) in saturation regime important in the consideration of an electrolyte solution in contact with charged surface (Gongadze, E. *et al*. Comput. Meth. Biomech. Biomed. Eng. submitted and Gongadze, E. and Iglič, A. Bioelectrochemistry submitted):

$$\varepsilon_r(x) = n^2 + n_s n_{0w} \frac{p_0}{\varepsilon_0} \left(\frac{2+n^2}{3}\right) \frac{\mathrm{F}\,(\gamma p_0 E\beta)}{\mathrm{D}\left(\phi, E\right) E}, \quad (39)$$

where

$$\mathrm{D}\left(\phi, E\right) = 2 n_0 \cosh(e_0 \phi\beta) + n_{0w} \frac{\sinh(\gamma p_0 E\beta)}{(\gamma p_0 E\beta)}, \quad (40)$$

$$\gamma = \frac{3}{2}\left(\frac{2+n^2}{3}\right). \quad (41)$$

In the limit of vanishing electric field strength the above Eq. 39 yields the Onsager expression for permittivity:

$$\varepsilon_r \approx n^2 + \left(\frac{2+n^2}{3}\right)^2 \frac{n_{0w} \beta p_0^2}{2\varepsilon_0}. \quad (42)$$

From Eq. 42 it follows that the value of the dipole moment p_0 = 3.1 D corresponds to the bulk permittivity $\varepsilon_r = 78.5$. This value is considerably smaller than the corresponding value in the LB model ($p_0 = 4.79$ D) (see Fig. 4) which does not take into account the cavity and reaction fields, and is also close to the experimental values of the effective dipole moment of water molecules in clusters ($p_0 = 2.7$ D) and in bulk solution ($p_0 = 2.4 - 2.6$ D). Nevertheless, this fact does not negate the predictions of the LB model where all the equations (including the expression for relative permittivity) have the same structure as in the modified LB model (i.e. in Eq. 39), only the effective value of water dipole moment p_0 is larger in LB model.

A practical application of the GSM developed can be found in the field of orthopaedics and specifically by surface modification of a hip implant. Namely, the cell and tissue reaction to the physical features of an implant surface ultimately determines the clinical success of an implant. The mechanism of the initial adhesion of osteoblastic cells to the implant surface is based on a protein and cation mediated attractive interaction between two negatively charged surfaces [25-27], i.e. the negatively charged implant surface and the negatively charged osteoblasts [28-30]. Therefore, the adhesion of osteoblasts to the implant is to a large extent determined by the electrical properties of the implant surface. Accordingly, many studies in the past indicated that increased negative surface potential of titanium implants promotes osteoblast adhesion and consequently, to new bone formation [29, 31, 32]. It it shown in this work that depletion and water ordering near the charged surface of a metal implant locally decrease the relative permittivity. The electric field strength and the magnitude of the negative electric potential in the close vicinity of the implant surface, due to this effect, are substantially increased which is of a crucial importance for the improved adhesion of cells to the metal surface [28, 29, 31, 32]. Accordingly, it has been shown recently that the topography of a nanostructured implant surface is a decisive factor for surface cell adhesion and growth [33-35]. The models of the electric double layer presented may thus serve as a practical tool to find the nanostructured surface topography of implants with optimal electric field strength and electric potential distribution that would promote the protein and cation mediated adhesion of osteoblasts to the negatively charged implant surface [35] and also communication between cells [36].

Acknowledgements. This work was supported by DFG for the project A3 in Research Training Group 1505/1 "*welisa*" (www.welisa.uni-rostock.de) and Slovenian Research Agency grants J3-9219-0381, P2-0232-1538.

REFERENCES

1. Helmholtz, H. Studien über elektrische Grenzschichten. **Ann. Phys.** 7 (1879) 337-382.
2. Gouy, M.G. Sur la constitution de la charge electrique à la surface d'un electrolyte. **J. Physique** (France) 9 (1910) 457-468.
3. Chapman, D.L. A contribution to the theory of electrocapillarity. **Philos. Mag.** 25 (1913) 475-481.
4. Stern, O. Zur Theorie der elektrolytischen Doppelschicht. **Z. Elektrochemie** 30 (1924) 508-516.
5. Manciu, M. and Ruckenstein, E. The polarization model for hydration/ double layer interactions: the role of the electrolyte ions. **Adv. Coll. Int. Sci.** 112 (2004) 109-128.
6. Gongadze, E., Bohinc, K., van Rienen, U., Kralj-Iglič, V. and Iglič, A. Spatial variation of permittivity near a charged membrane in contact with electrolyte solution, in: **Advances in planar lipid bilayers and liposomes** (Iglič, A. Ed.) 11th volume, Elsevier, 2010, 101-126.
7. Gongadze, E., van Rienen, U., Kralj-Iglič, V. and Iglič, A. Langevin Poisson-Boltzmann equation: point-like ions and water dipoles near charged membrane surface. **Gen. Physiol. Biophys.** 30 (2011) 130-137.
8. Outhwaite CW. Towards a mean electrostatic potential treatment of an ion-dipole mixture or a dipolar system next to a plane wall. **Mol. Phys.** 48 (1983) 599-614.
9. Bazant, M.Z., Kilic, M.S., Storey, B. and Ajdari, A. Towards an understanding of induced-charge electrokinetics at large applied voltages in concentrated solutions. **Adv Coll. Int. Sci.** 152 (2009) 48-88.
10. Jackson, J.D. **Classical electrodynamics.** 3rd edition, Wiley and Son Inc., 1998.
11. Butt, H. J., Graf, K. and Kappl, M. **Physics and chemistry of interfaces**. 1st edition, Wiley-VCH Verlag, 2003.
12. McLaughlin, S. The electrostatic properties of membranes. **Ann. Rev. Biophys. Chem.** 18 (1989) 113-136.
13. Bikerman, J.J. Structure and capacity of the electrical double layer. **Phil. Mag.** 33 (1942) 384-397.
14. Kralj-Iglič, V. Free energy of the electric double layer within the approximation of high electrolyte concentration. **Electrotechnical Rev.** 62 (1995) 104-108.
15. Kralj-Iglič, V. and Iglič A. A simple statistical mechanical approach to the free energy of the electric double layer including the excluded volume effect. **J. Phys. II** 6 (1996) 477-491.
16. Lamperski, S. and Outhwaite, C.W. Exclusion volume term in the inhomogeneous Poisson-Boltzmann theory for high surface charge. **Langmuir** 18 (2002) 3423-3424.

17. Iglič, A., Gongadze, E. and Bohinc, K. Excluded volume effect and orientational ordering near charged surface in solution of ions and Langevin dipoles. **Bioelectrochemistry** 79 (2010) 223-227.
18. Adams, D.J. Theory of the dielectric constant of ice. **Nature** 293 (1981) 447-449.
19. Dill, K.A. and Bromberg S. **Molecular driving forces**. Garland Science, 2003.
20. Fröhlich, H. Theory of dielectrics. Clarendon Press, 1964.
21. Franks, F. **Water. A comprehensive treatise**, vol. 1, The physics and physical chemistry of water, Plenum Press, 1972
22. Onsager, L. Electric moments of molecules in liquids. **J. Am. Chem. Soc.** 58 (1936) 1486-1493.
23. Kirkwood, J.G. The dielectric polarization of polar liquids. **J. Chem. Phys.** 7 (1939) 911-919.
24. Booth, F. The dielectric constant of water and the saturation effect. **J. Chem. Phys.** 19 (1951) 391-394.
25. Urbanija, J., Bohinc, K., Bellen, A., Maset, S., Iglič, A., Kralj-Iglič, V. and Kumar, P.B.S. Attraction between negatively charged surfaces mediated by spherical counterions with quadrupolar charge distribution. **J. Chem. Phys.** 129 (2008) 105101.
26. Frank, M., Sodin-Šemrl, S., Rozman, B., Potočnik, M. and Kralj-Iglič, V. Effects of low-molecular-weight heparin on adhesion and vesiculation of phospholipid membranes - a possible mechanism for the treatment of hypercoagulability in antiphospholipid syndrome. **Ann. N. Y. Acad. Sci.** 1173 (2009) 874-886.
27. Zelko, J., Iglič, A., Kralj-Iglič, V. and Kumar, P.B.S. Effects of counterion size on the attraction between similarly charged surfaces. **J. Chem. Phys.** 133 (2010) 204901.
28. Kabaso, D., Gongadze, E., Perutkova, Š., Kralj-Iglič, V., Matschegewski, C., Beck, U., van Rienen, U. and Iglič, A. Mechanics and electrostatics of the interactions between osteoblasts and titanium surface. **Comput. Meth. Biomech. Biomed. Eng.** 14 (2011) 469-482.
29. Smeets, R., Kolk, A., Gerressen, M., Driemel, O., Maciejewski, O., Hermanns-Sachweh, B., Riediger, D. and Stein J. A new biphasic osteoinductive calcium composite material with a negative zeta potential for bone augmentation. **Head Face Med.** (2009) Available from: 5: 13 doi: 10.1186/1746-160X-5-13.
30. Heath, M.D., Henderson, B. and Perkin S. Ion-specific effects on the interaction between fibronectin and negatively charged mica surfaces. **Langmuir** 26 (2010) 5304-5308.
31. Teng, N.C., Nakamura, S., Takagi, Y., Yamashita, Y., Ohgaki, M. and Yamashita K. A new approach to enhancement of bone formation by electrically polarized hydroxyapatite. **J. Dent. Res.** 80 (2000) 1925-1929.

32. Oghaki, M., Kizuki, T., Katsura, M. and Yamashita K. Manipulation of selective cell adhesion and growth by surface charges of electrically polarized hydroxyapatite. **J. Biomed. Mater. Res.** 57 (2001) 366-373.
33. Park, J., Bauer, S., Schlegel, K., Neukam, F., Mark, K. and Schmuki, P. TiO2 nanotube surfaces: 15 nm - an optimal length scale of surface topography for cell adhesion and differentiation. **Small** 5 (2009) 666-671.
34. Puckett, S., Pareta, R. and Webster T. Nano rough micron patterned titanium for directing osteoblast morphology and adhesion. **Int. J. Nanomedicine** 3 (2008) 229-241.
35. Gongadze, E., Kabaso, D., Bauer, S., Slivnik, T., Schmuki, P., van Rienen, U., Iglič, A. Adhesion of osteoblasts to a nanorough titanium implant surface. **Int. J. Nanomedicine** 6 (2011) in press
36. Schara, K., Janša, V., Šuštar, V., Dolinar, D., Pavlič, J.I., Lokar, M., Kralj-Iglič, V., Veranič, P., Iglič, A. Mechanisms for the formation of membranous nanostructures in cell-to-cell communication. **Cell. Mol. Biol. Lett.** 14 (2009) 636-656.